Solid State Ionics xxx (2015) xxx–xxx

Contents lists available at ScienceDirect

Solid State Ionics

journal homepage: www.elsevier.com/locate/ssi

$Ce(Mn,Fe)O_2$–$(La,Sr)(Fe,Mn)O_3$ composite as an active cathode for electrochemical reduction of CO_2 in proton conducting solid oxide cells

Tae Ho Shin [a,*,1,2], Jae-ha Myung [a,1], Khan M. Naeem [a,b], Cristian Savaniu [a], John T.S. Irvine [a,*]

[a] School of Chemistry, University of St Andrews, St Andrews, Scotland, United Kingdom
[b] Centre of Advanced Materials and Energy Studies (CAMES), University Brunei Darussalam, Brunei

ARTICLE INFO

Article history:
Received 12 December 2014
Received in revised form 24 February 2015
Accepted 11 March 2015
Available online xxxx

Keywords:
Solid oxide electrolyser
Composite cathode
CO_2 reduction
Proton conductor
Ceria

ABSTRACT

A solid oxide electrolysis cell concept for reducing CO_2 to CO was studied using a proton conducting mixed oxide — $BaCe_{0.7}Zr_{0.1}Y_{0.1}Yb_{0.06}Zn_{0.04}O_{3-\delta}$ (BCZYYZ) as an electrolyte. The oxide composite mixture: $Ce_{0.6}Mn_{0.3}Fe_{0.1}O_2$–$La_{0.6}Sr_{0.4}Fe_{0.9}Mn_{0.1}O_3$ (12.5–87.5 wt.%) was examined as enhancing catalyst electrode for CO_2 reduction and proton oxidation reaction on the cathode side for avoiding coke formation. Here we demonstrate the successful electrochemical reduction of CO_2 in proton conducting SOECs. During electrochemical reduction of CO_2 at 700 °C, current densities as high as 0.5 A/cm^2 and 1 A/cm^2 at 1.3 V and 2.2 V respectively, were withdrawn even though the cell employed a 400 μm thick BCZYYZ electrolyte support.

1. Introduction

Development of new energy sources such as solar and wind, giving a rich and diverse energy supply based upon renewable and environmentally friendly sources, has emphasized the need for new methods of energy storage. Recently, there has been an increased focus on hydrogen as an alternative energy mediator of conversion and storage because of high gravimetric energy density and zero carbon emission [1–5]. However, the utilisation of hydrogen has been limited due to the practical engineering and economic limitations with respect to its generation and distribution [6]. On the other hand hydrocarbon fuels and carbon monoxide match the existing energy infrastructure well because of their similarity to current fossil fuels; they would be effective energy carriers in a period of transition toward zero carbon emission [7–9]. The synthetic hydrocarbon fuels from CO_2/H_2O with renewable electricity have therefore been proposed as an alternative method to transport new energy sources from where they are available to its point of use within a carbon neutral cycle [10–13]. In addition, using electrochemical reaction for recycling or reuse of CO_2 from new energy sources would therefore be a feasible alternative to advanced capture and utilisation of CO_2.

A proton conducting solid oxide electrolyser has recently been applied for electrolysis of water combined with electrochemical conversion of CO_2 [13–16]. Using a proton conducting oxide as electrolyte in CO_2 condition, it is possible to produce hydrogen from steam while simultaneously reducing CO_2 to generate hydrocarbon such as methane as illustrated in Fig. 1. Xie et al. have demonstrated the successful in-situ electrochemical conversion of H_2O/CO_2 into methane at 650 °C from 1 to 2% of CO_2 in previous work [13]. At the cathode side, if CO_2 is fed then reverse water gas shift reaction (WGSR) would take place following the overall cathode reaction.

$$CO_2 + 4H^+ + 4e^- \leftrightarrow CO + 2H_2O \quad (1)$$

If the partial pressure of CH_4 at equilibrium is low, however, most the CO_2 would be converted into CO. In the case of the proton conducting solid oxide cell, the electrochemical reaction would be mainly dominated by the cathode reaction. Thus, the cathode should require good properties in terms of electrical conductivity as well as catalytic activity for hydrocarbon formation. Furthermore, carbon tolerance would be one of the important issues because carbon deposition is likely to occur at the cathode side during CO_2 reduction. In the present work, the mixed oxide composite with $Ce(Mn, Fe)O_2$–$(La,Sr)(Fe,Mn)O_3$ (CMF–LSFM) was employed as a catalyst coating layer on the cathode side in proton conducting solid oxide cells to facilitate catalysis and electrochemical electrode reaction with pure CO_2 gas. The CMF–LSFM composite oxide previously showed outstanding catalytic activity for fuel oxidation without carbon coking in the hydrocarbon-type solid oxide fuel cells as an oxide anode [17,18]. Compare to the typical

* Corresponding authors at: School of Chemistry, University of St Andrews, St Andrews, Fife, Scotland KY16 9ST, United Kingdom.
E-mail addresses: ths@st-andrews.ac.uk, ceramist95@gmail.com (T.H. Shin), jtsi@st-andrews.ac.uk (J.T.S. Irvine).
[1] These authors contributed equally to this work as first author.
[2] This author's affiliation has been changed to Korea Institute of Ceramic Engineering Technology (KICET).

http://dx.doi.org/10.1016/j.ssi.2015.03.015

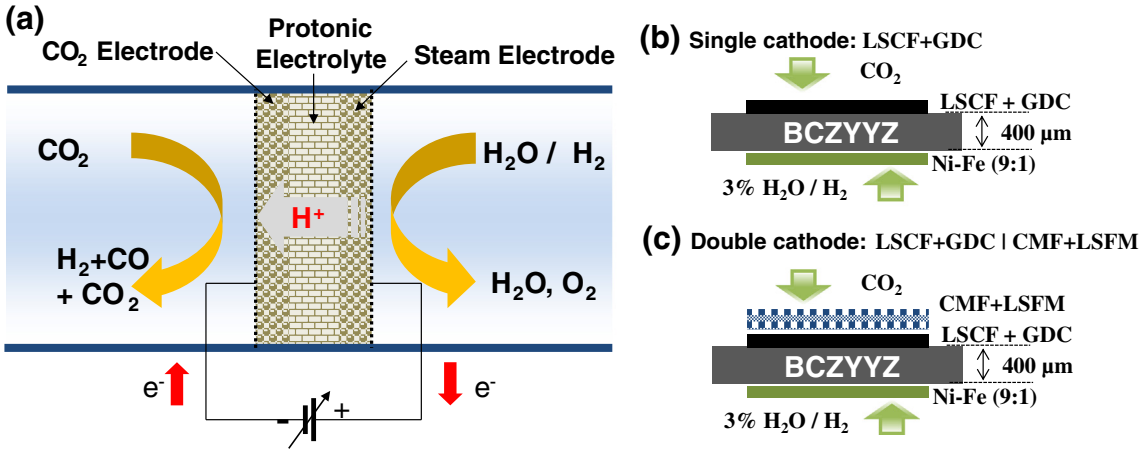

Fig. 1. a) Schematic diagram of CO_2 reduction in proton conductor. b) Cell configuration using single cathode layer, LSCF + GDC and c) double cathode layers, LSCF + GDC|CMF + LSFM.

cathode materials, (La,Sr)(Fe,Co)O_3–Gd doped ceria (GDC) cathode in proton conducting electrolyser, CMF–LSFM has an improved catalytic activity for CO_2 electro-conversion with a smaller overpotential loss.

2. Experimental

$Ce_{0.6}Mn_{0.3}Fe_{0.1}O_2$ and $La_{0.6}Sr_{0.4}Fe_{0.9}Mn_{0.1}O_3$ mixed oxides were prepared using the conventional solid-state reaction method described in detail previously [18]. The powders were mixed under acetone in an agate mortar to form a composite oxide anode consisting of 12.5 wt.% Ce(Mn, Fe)O_2 and 87.5 wt.% La(Sr)Fe(Mn)O_3. $BaCe_{0.7}Zr_{0.1}Y_{0.1}Yb_{0.06}Zn_{0.04}O_{3-\delta}$ (BCZYYZ) powder was synthesized by a modified glycine-nitrate combustion method. $Ba(NO_3)_2$ (98.0%, Sigma-Aldrich Co. LLC, UK), $Ce(NO_3)_3 \cdot 6H_2O$(99.0%, Sigma-Aldrich Co. LLC, UK), $ZrO(NO_3)_2 \cdot \chi H_2O$, $Y(NO_3)_3 \cdot 6H_2O$ (99.0%, Sigma-Aldrich Co. LLC, UK), and $Zn(NO_3)_2 \cdot 6H_2O$(98.0%, Sigma-Aldrich Co. LLC, UK) were added in the corresponding ratios into distilled water containing an appropriate amount of citric acid (4:1 to metal ions) in a beaker under stirring until a transparent and homogeneous solution was obtained. The solution was evaporated on the hotplate and resulting powder was calcined at 1000 °C for crystallisation. The BCZYYZ electrolyte support was prepared by dry-pressing powder into a circular green body followed by a high-temperature sintering in air at 1450 °C for 6 h and mechanical polishing until 2 cm diameter and 400 μm thickness electrolyte supports were obtained. The faces of the BCZYYZ electrolyte disk were coated with the corresponding electrode powder by screen-printing, and then electrodes were sintered at 1100 °C for 30 min. To compare with conventional $La_{0.6}Sr_{0.4}Fe_{0.8}Co_{0.2}O_3$ (LSCF)–Gd doped ceria (GDC) commercial cathode, the CMF–LSFM coating layer (<5 μm thickness) was just added on top of the same LSCF–GDC cathode in another single cell, Ni–Fe|BCZYYZ|LSCF–GDC|CMF-LSF. Ni–Fe (9:1) alloy powder was used for anode, coated using screen printing. To minimize changing the geometric factor from adding CMF–LSFM layer by screen printing, coating layer was prepared as thin (<5 μm) as possible. A gold spot electrode prepared using commercial Au paste was used as the reference electrode and was placed on the cathode side. We connected gold lead wire to the reference electrode.

To evaluate electrochemical properties, I–V curves and impedance were measured with four silver leads with silver mesh as the electrode current collector. In order to perform electrochemical testing in fuel cell mode, humidified H_2 was supplied into the Ni–Fe electrode while the cathode side was exposed to air as an oxidant gas. After fuel cell mode test, 3 vol.% H_2O/H_2 and 100% CO_2 were supplied into the anode and cathode while external loading was also applied to perform the electrochemical test for CO_2 reduction. AC impedance spectroscopy was recorded using an IM6 Electrochemical Workstation (Zahner, Germany) with frequency ranged from 0.1 Hz to 100 kHz with amplitude of 10 mV.

3. Results and discussion

Fig. 2 shows the microstructure of the CMF–LSFM catalyst layer on top of the LSCF–GDC cathode layer together with the BCZYYZ electrolyte support after electrochemical measurement. The adherence of the electrolyte, cathode and functional catalyst layers is very good and no delamination is observed even after the cell test. In addition, there was no evidence for carbon deposition in cathode side during CO_2 reduction. It is well known that a coke deposited resulted from CO_2/CO gas utilisation would appear as filament-like structures, leading to catalyst deactivation. The absence of these structures suggests carbon tolerance of the CMF–LSFM in CO_2 atmosphere, expected from previous reports on the CMF–LSFM composite SOFC anode [17].

To verify the influence of CMF–LSFM upon the catalytic activity of the LSCF–GDC cathode layer, electrochemical tests were performed on cells comprising Ni:Fe anode, BCZYYZ electrolyte (400 μm thick) and LSCF–GDC cathode with and without the added CMF–LSFM functional layer. Fig. 3 shows the current–power density (I–P) and current–voltage (I–V) curves of the cell using the LSCF–GDC cathode and CMF–LSFM/LSCF–GDC dual cathode cell configurations. The open circuit voltage (OCV) in humidified H_2 fuel were close to the value predicted by the Nernst equation, 1.061, 1.088, and 1.112 V at 800, 700, and 600 °C, respectively, for the cells having LSCF–GDC cathode. On the other hand, the OCV of the cell with added CMF-LSFM catalyst layer on the LSCF–GDC cathode was slightly lower than that of the cell using only LSCF–GDC cathode, 1.02, 1.066 and 1.102 V at 800, 700, and 600 °C, respectively. According to previous literature for $BaCeO_3$ proton conductor, partial oxygen conduction would clearly occur at high temperature (>700 °C) and high oxygen partial pressure [19]. However, the BCZYYZ electrolyte supporting cells were exposed to both high oxygen condition (oxidant electrode) and lower oxygen condition (fuel electrode) in real fuel cell operation mode. Thus, OCV value would be more realistic information to check partial oxygen conduction in proton electrolyte during operation rather than theoretical proton transport number. Obviously, all of OCV values are over 1 V, which is closed to theoretical value within whole temperature range (600–800 °C) and OCV of ca. 1.1 V was particularly recorded at 600 °C as shown in Fig. 3. It was observed that the introduction of the CMF–LSFM functional layer on the cathode side almost doubled the maximum power density value (MPD) as can be seen from Fig. 3(a) and (b), suggesting that not only catalytic surface activity would be improved by CMF–LSFM, but also the charge transfer is facilitated in the CMF–LSFM catalytic functional layer because of its mixed

Please cite this article as: T.H. Shin, et al., Solid State Ionics (2015), http://dx.doi.org/10.1016/j.ssi.2015.03.015

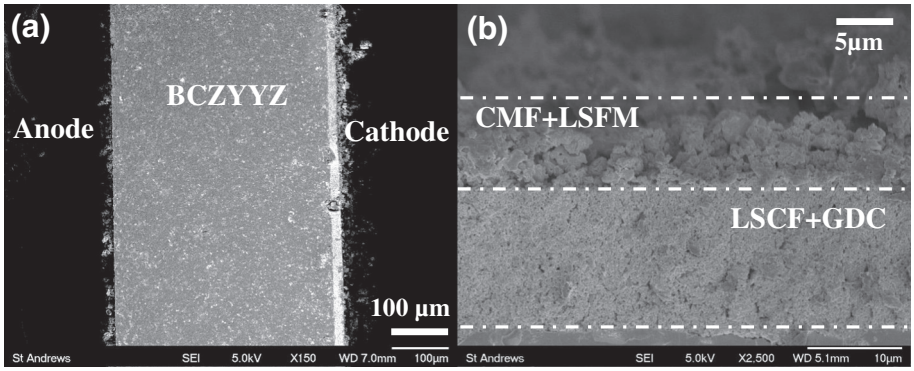

Fig. 2. SEM images of a cell using double cathode: LSCF + GDC|CMF + LSFM, on BCZYYZ electrolyte support after electrochemical test, a) cross section, and b) high magnification.

ionic–electronic conduction properties. ASR values determined from the I–V curves are 2.80 and 2.06 Ω cm^2 for the cell using only LSCF–GDC cathode and additional CMF–LSFM layer at 700 °C, respectively. Impedance spectroscopy data were obtained during the fuel cell tests and helped shedding more light on this last point. Fig. 4 shows the typical impedance plots for Ni–Fe|BCZYYZ|LSCF–GDC compared to the Ni–Fe|BCZYYZ|LSCF–GDC|CMF–LSF cell configuration at 700 °C, under OCV conditions. The intercept with the real axis at high frequencies represents the cell's ohmic resistance (Rs), whereas the difference between the high and lower frequency responses (semicircles) with the real axis presents the sum of the polarisation resistance (Rp). The CMF–LSFM containing cell presented a lower polarisation resistance value than that of only LSCF–GDC cathode cell, in agreement with the ASR values extracted from the I–V curves shown in Fig. 3, since ohmic resistance of the CMF–LSFM containing cell was slightly larger due to its lower electrical conductivity. However, ohmic resistances (Rs ≈ 2.2 Ω cm^2 at 700 °C) would be almost dominated by electrolyte conductivity and consequently Rs values were very closed to theoretical value (≈2.2 Ω cm^2), considering conductivity of the BCZYYZ at 700 °C (σ ≈ 0.018 Ω^{-1} cm^{-1} at 700 °C, R_{ohmic} = thickness/(σ·area)). In any case, it is reasonable to assume that the lower value obtained for the electrochemical reaction resistance by adding the catalyst layer, CMF–LSFM, was due to the improved catalytic activity of CMF–LSFM material that makes it suitable for proton conducting fuel cells.

Furthermore, in order to verify the electrochemical reduction of CO_2, we replaced the air feeding the cathode side of the electrochemical cell with pure CO_2 gas, monitoring the cell performance. Fig. 5(a) shows the electrochemical performance in CO_2 for Ni–Fe|BCZYYZ|LSCF–GDC cell compared to the cell where CMF–LSFM was added (Ni–Fe|BCZYYZ|LSCF–GDC|CMF–LSFM), at 700 °C. As in the previous case, the current density was significantly improved by introducing CMF–LSFM as 0.5 A/cm^2 were achieved at 1.3 V in this case compared to 0.18 A/cm^2 measured with the LSCF–GDC cathode only. This confirms that CMF–LSFM catalyst layer has also positive effects for the CO_2 reduction reaction in a proton conducting electrolysing cell; thus, the cell with the CMF–LSFM active layer exhibits a much smaller polarisation resistance value than that of only LSCF–GDC cathode

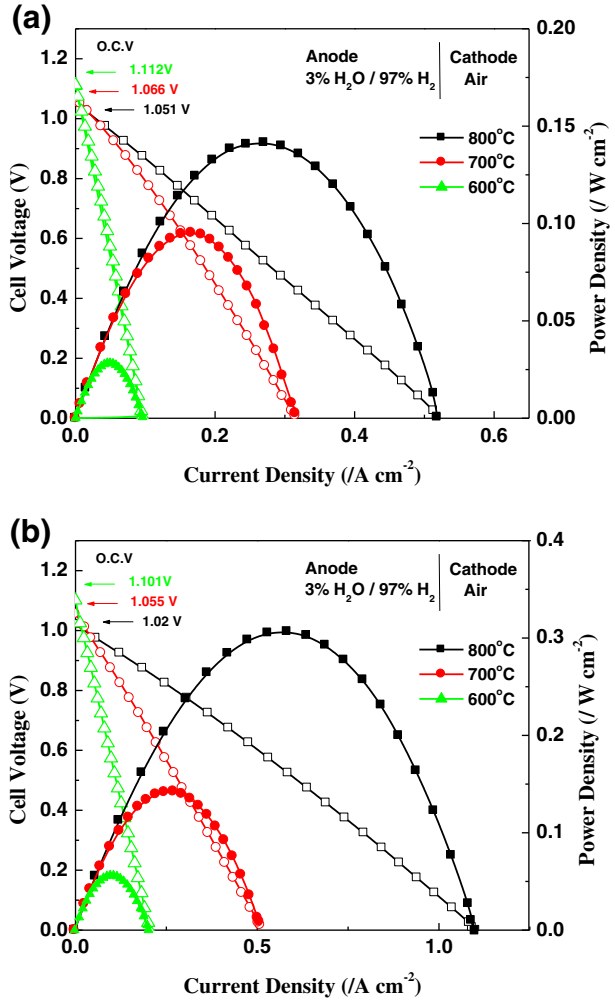

Fig. 3. I–V curves and corresponding power density curve for a) the cell using single cathode, Ni–Fe|BCZYYZ|LSCF–GDC, and b) double cathode, Ni–Fe|BCZYYZ|LSCF–GDC|CMF–LSFM.

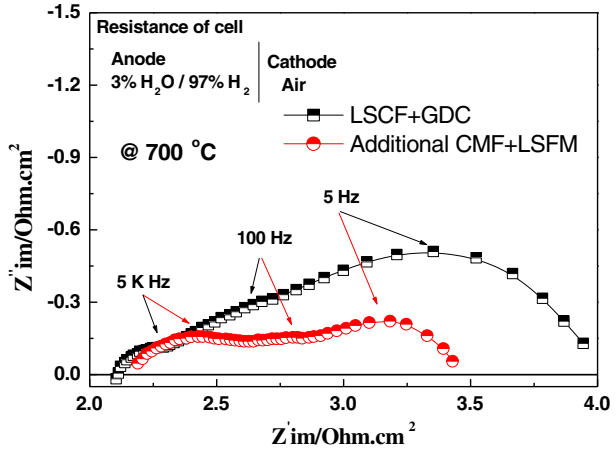

Fig. 4. Impedance spectra of the cells: using single cathode, Ni–Fe|BCZYYZ|LSCF–GDC, and double cathode, Ni–Fe|BCZYYZ|LSCF–GDC|CMF–LSFM under open current condition at 700 °C.

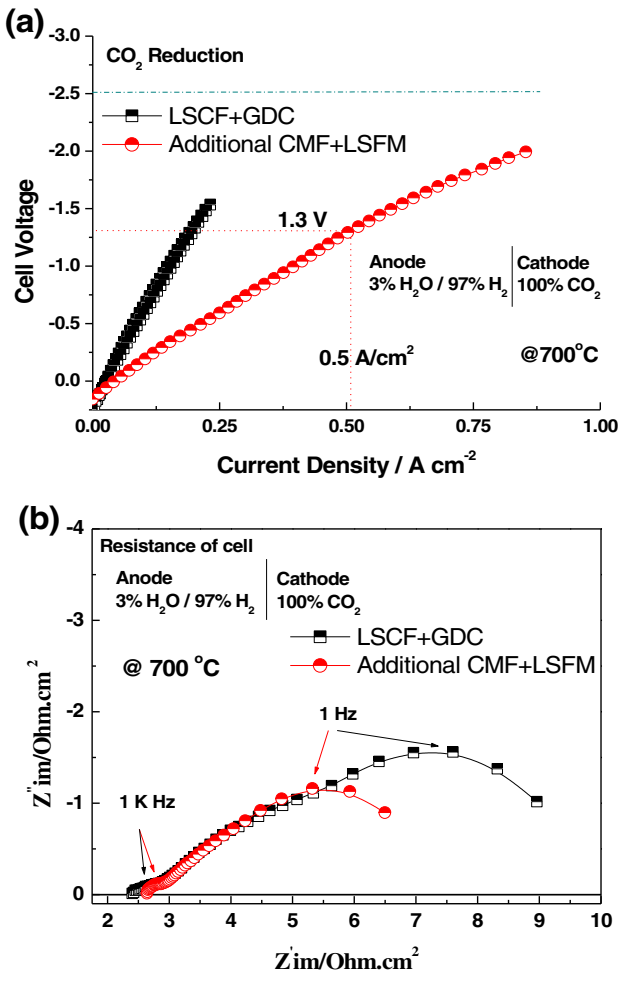

Fig. 5. I–V curves of CO_2 reduction in proton conductor cells: using single cathode, Ni–Fe|BCZYYZ|LSCF–GDC, and double cathode, Ni–Fe|BCZYYZ|LSCF–GDC|CMF–LSFM under open current condition at 700 °C.

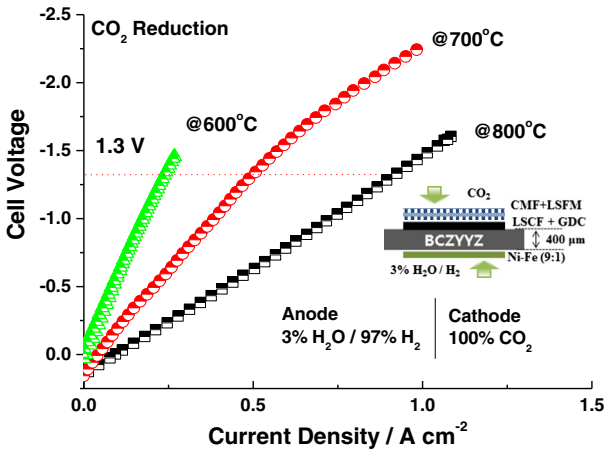

Fig. 6. I–V curves of CO_2 reduction in proton conductor cells double cathode, Ni–Fe|BCZYYZ|LSCF–GDC|CMF–LSFM under open current condition as function of operation temperature.

cell as shown in Fig. 5(b), in agreement with the value obtained from the I–V curves. We previously reported the analysis of the gas composition during electrochemical testing of similar cells, showing a mixture of syngas and CH_4 (1.2%), with a CO concentration of 61% (produced at the rate of 3.25 ml/min cm^2) and the corresponding CO_2 conversion of around 65% [13]. Here, the exhaust gases are expected to have similar composition to the one reported in the previous study because the current and voltage values (1.3 V, 0.25 A/cm^2 at 600 °C in Fig. 6) are very similar to the ones obtained before, were strong evidence of CO_2 reduction and methane production was demonstrated. However, detailed analysis of gas products during the transient period is now under study, and the results will be reported in a future report. Fig. 6 summarises the I–V curve for the electrochemical reduction of CO_2 in the CMF–LSFM added (Ni–Fe|BCZYYZ|LSCF–GDC|CMF–LSFM), proton solid oxide cells, with 3% H_2O/H_2 fuel and 100% CO_2 on anode and cathode sides, respectively, at different temperatures. The absolute open circuit voltages were around −0.157 V at 700 °C coming from the pre-reduced electrode in small oxygen partial pressure of pure CO_2 gas. The superior performance obtained with the CMF–LSFM active cathode layer is very encouraging for further development and utilisation of these cells in a different design and at a larger scale.

4. Conclusions

In this work, a proton-conducting solid oxide cell with the configuration, Ni–Fe|BCZYYZ|LSCF–GDC|CMF–LSFM, was demonstrated for the efficient electro-conversion of H_2O/CO_2, demonstrating that the electrochemical performance was improved by CMF–LSFM addition to the cathode as a catalyst layer. The I–V curves in the SOFC and CO_2 reduction modes exhibited higher current density when the CMF–LSFM catalyst layer was present, accompanied by a significant decrease in polarisation resistance of the cell. During CO_2 reduction at 700 °C, current density values as high as 0.5 A/cm^2 and 1 A/cm^2 were obtained at 1.3 V and 2.2 V respectively, even with relatively thick BCZYYZ electrolyte supports (ca. 400 μm). Furthermore, no carbon deposition was evident after the CO_2 reduction of test when pure CO_2 was used at the air electrode side. Therefore, the electrochemical reduction of CO_2 in proton conducting solid oxide electrolyser using a CMF–LSFM catalyst layer would be an attractive option for cycling CO_2 since reasonably high current density was achieved.

Acknowledgements

We thank EPSRC (EP/I022570/1, EP/K015540/1, EP/I038950/1) and the Royal Society (WRMA 2012/R2) (Wolfson Research Merit award) for support. We thank also the In-house Program (2E24842) of the Korea Institute of Science and Technology (KIST), Republic of Korea for support.

References

[1] J.L. Bernal-Agustín, R. Dufo-López, Int. J. Hydrog. Energy 33 (2008) 6401–6413.
[2] J.O.M. Bockris, T.N. Veziroglu, Int. J. Hydrog. Energy 32 (2007) 1605–1610.
[3] S.H. Jensen, P.H. Larsen, M. Mogensen, Int. J. Hydrog. Energy 32 (2007) 3253–3257.
[4] W. Doenitz, R. Schmidberger, E. Steinheil, R. Streicher, Int. J. Hydrog. Energy 5 (1980) 55–63.
[5] A.O. Isenberg, Solid State Ionics 3–4 (1981) 431–437.
[6] E.H. Seymour, L. Murray, R. Fernandes, Int. J. Hydrog. Energy 33 (2008) 3015–3020.
[7] L. Schlapbach, Nature 460 (2009) 809–811.
[8] L. Wang, R.T. Yang, Energy Environ. Sci. 1 (2008) 268–279.
[9] B. Sakintuna, F. Lamari-Darkrim, M. Hirscher, Int. J. Hydrog. Energy 32 (2007) 1121–1140.
[10] S.D. Ebbesen, M. Mogensen, J. Power Sources 193 (2009) 349–358.
[11] N.Q. Minh, M.B. Mogensen, Electrochem. Soc. Interface 22 (2013) 55–62.
[12] C. Graves, S.D. Ebbesen, M. Mogensen, Solid State Ionics 192 (2011) 398–403.
[13] K. Xie, Y. Zhang, G. Meng, J.T.S. Irvine, J. Mater. Chem. 21 (2011) 195–198.
[14] E. Ruiz-Trejo, J.T.S. Irvine, Solid State Ionics 252 (2013) 157–164.
[15] S. Wang, H. Tsuruta, M. Asanuma, T. Ishihara, Adv. Energy Mater. 5 (2014) 1401003–1401013.
[16] S. Wang, A. Inoishi, J.-e. Hong, Y.-w. Ju, H. Hagiwara, S. Ida, T. Ishihara, J. Mater. Chem. A 1 (2013) 12455–12461.
[17] T.H. Shin, S. Ida, T. Ishihara, J. Am. Chem. Soc. 133 (2011) 19399–19407.
[18] T.H. Shin, P. Vanalabhpatana, T. Ishihara, J. Electrochem. Soc. 157 (2010) B1896–B1901.
[19] M. Oishi, S. Akoshima, K. Yashiro, K. Sato, J. Mizusaki, T. Kawada, Solid State Ionics 179 (2008) 2240–2247.